Chapter 6
Fast Switching Behavior in Nonlinear Electronic Circuits: A Geometric Approach

Tina Thiessen, Sören Plönnigs, and Wolfgang Mathis

Abstract. In this paper an outline about the geometric concept of nonlinear electronic circuits is given. With this geometric concept the fast switching behavior of circuits, i.e. the jumps in their state space, is illustrated and a jump condition is formulated. Furthermore, the developed geometric approach is adapted to MNA based systems of equations. This new method enables the simulation of such ill-conditioned circuits without regularization and presents an implementation approach for common circuit simulators like SPICE.

6.1 Introduction and Motivation

Circuit simulation is a key tool in the design of electronic circuits. Despite the successful development on the construction of robust circuit simulators [1], there are still some open problems, e.g. the simulation of fast switching behavior in nonlinear circuits.

Interesting circuits for our purpose are circuits with fast switching behavior, i.e. circuits with discontinuous changes, which are called ”jumps” in state space. Attributes which indicate fast switching behavior are for example topological properties like positive feedback and circuit characteristics like negative differential resistance or port characteristics seen by capacitors and inductors. It is mentionable that many so-called digital circuits belong to these class of circuits, because they are in fact analog circuits that retain information by assuming a certain state. When the information changes, fast transitions may occur. One can show, that those non-regularized circuits contain a “fold” in their manifolds (see Fig. 6.1) and provide examples for the so-called “time-constant problem” of circuit simulation (see [2], [3]).

Tina Thiessen · Sören Plönnigs · Wolfgang Mathis
Institute of Theoretical Electrical Engineering, Leibniz University of Hanover,
D-30167, Hanover, Germany
e-mail: {thiessen,ploennigs,mathis}@tet.uni-hannover.de

K. Kyamakya et al. (Eds.): Selected Topics in Nonlinear Dynamics, SCI 459, pp. 99–116.
DOI: 10.1007/ 978-3-642-34560-9_6

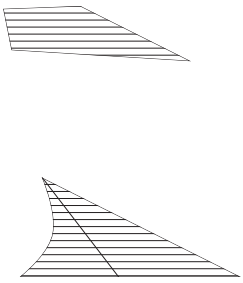

Fig. 6.1 Folded state space of non regularized network

It can be shown, that the simulation with common circuit simulators of non-regularized networks $\mathcal{N}$ fails, if their state space $\mathcal{S}$ exhibits a fold with respect to a network specific projection direction and if the dynamics is in the vicinity of the fold edge (cf. Fig. 6.1: fold edge is represented by the edge of the shaded area). Such a fold leads to jumps in the embedding space from one point on $\mathcal{S}$ to another, which corresponds to the fast switching in the transient solutions. The points during the jump are no admitted points, because they are outside $\mathcal{S}$. Therefore, we need to introduce an embedding space $\mathcal{E} = \mathbb{R}^k$ and where $\mathcal{S}$ is a subset of $\mathcal{E}$. When the network is ϵ-regularized [4], the jump behavior can be viewed as the limit $\epsilon \to 0$ of the solutions of the singularly perturbed system [5]. The state space $\mathcal{S}_\epsilon$ of the regularized network $\mathcal{N}_\epsilon$ is defined in a different embedding space $\mathcal{E}_\epsilon = \mathbb{R}^{k+c}$ and contains parts of $\mathcal{S}$. However, the fold edge of $\mathcal{S}$ marks - in particular for $\epsilon \to 0$ - the ill-conditioned areas of the dynamics of $\mathcal{N}_\epsilon$. This fold edge corresponds also to the impasse points described in [6], [7]. By adding suitably located ϵ-parasitic inductors L or capacitors C considering Tikhonov's Theorem [8], the network is regularized [9]. Nevertheless, by choosing wrongly located L's and C's, the circuit can be regularized indeed, but the determined transient solutions are inconsistent with respect to $\mathcal{N}$. Another problem are the widely spaced time-constants, which appear due to the fact that the dynamics of a regularized circuit can be divided into a slow and a fast part, leading to the so-called "time-constant problem" of circuit simulation [2]. This difficulty can be circumvented by using stiff solvers (e.g. implicit integration methods like BDF or Gear method) if the reason for the time-constant problem is not related to a jump behavior [3]. In previous publications [10], [11], we have shown the implementation of a geometric concept using geodetic differential equations. In this work we will, for the first time, adapt an alternative geometric concept to systems of equations based on the Modified Nodal Analysis (MNA).

6.2 Geometric Approach of Circuits and Fast Switching Behavior

It is known that the state space $\mathcal{S}$ of an electronic circuit can be interpreted as a differential manifold [12]. The branch voltages and currents must satisfy the algebraic nonlinear resistive and Kirchhoff constraints. The Kirchhoffian space $\mathcal{K}$ is defined as the set of all currents and voltages which satisfies Kirchhoff's laws. Moreover the Ohmian space $\mathcal{O}$ is defined as the set of all currents and voltages which satisfies all resistive constitutive relations. Thus the state space of the circuit is defined as the intersection of the Ohmian space $\mathcal{O}$ and the Kirchhoffian space $\mathcal{K}$ by $\mathcal{S} := \mathcal{K} \cap \mathcal{O}$ [13], [14].
The dynamics of a nonlinear dynamic circuit are defined by the set of all solutions of the descriptive differential equations on a sufficient smooth state space $\mathcal{S}$. Therefore the following conditions have to be fulfilled: 1) $\mathcal{S}$ is a smooth manifold. 2) The dynamics can be created on $\mathcal{S}$.

A set possesses the structure of a differentiable (smooth) m-dimensional manifold if it is locally equivalent to a $\mathbb{R}^m$. A concrete representation of a manifold can be given by means of a chart (map) that maps a part of $\mathcal{S}$ into $\mathbb{R}^m$. A detailed discussion about differentiable manifolds can be found in the monograph of Guillemin and Pollack [15].
The Kirchhoffian space $\mathcal{K}$ has a vector space structure in linear and nonlinear circuits since Kirchhoff's laws are homogeneous equations. Therefore $\mathcal{K}$ has also the structure of a differentiable manifold. But in general the Ohmian space $\mathcal{O}$ is not a differentiable manifold and even if $\mathcal{O}$ wears the structure of a differentiable manifold it is not obvious that the state space $\mathcal{S}$ wears this structure.
If we consider a circuit by its descriptive equations it means that the intersection of the solution sets of the Kirchhoffian equations and the Ohmian equations is a smooth manifold if these equations are "local" independent. From a geometric point of view this means that the intersection of $\mathcal{K}$ and $\mathcal{O}$ is "transversal" or in a more technical setting: if $\mathcal{K}$ and $\mathcal{O}$ are two submanifolds of $\mathbb{R}^{2n}$ (where n is the number of branches) we call $\mathcal{K}$ and $\mathcal{O}$ transversal, if the following condition is satisfied:

$$x \in \mathcal{K} \cap \mathcal{O} \text{ where } T_x\mathcal{K} \oplus T_x\mathcal{O} = T_x\mathbb{R}^{2n} \text{ or } x \notin \mathcal{K} \cap \mathcal{O} \tag{6.1}$$

Now, we are able to characterize the standard situation in nonlinear dynamical circuits. The state space $\mathcal{S}$ is a smooth manifold if: 1) the Ohmian space $\mathcal{O}$ is a smooth manifold and 2) the state space $\mathcal{S} = \mathcal{K} \cap \mathcal{O}$ is not empty as well as $\mathcal{K}$ and $\mathcal{O}$ are transversal. These properties can be satisfied by applying a suitable remodelling technique with resistive elements [16]. Therefore, this situation is typical or so-called generic and in the following we assume $\mathcal{S}$ to be a smooth manifold.

The second condition requires the construction of a vector field X on the smooth manifold $\mathcal{S}$. We know that based on fundamental physical laws, the relationships between currents and voltages of λ capacitors and γ inductors are given by means of differential relations. Therefore these differential equations are formulated in i_L and u_C coordinate planes $\mathbb{R}_i^\lambda \oplus \mathbb{R}_u^\gamma$ of the embedding space $\mathbb{R}^{2n}$.

We define a 1-form Ω and a 2-form G on the space of currents of inductors and voltages of capacitors. Then a projection map $\pi\colon \mathcal{S} \to \mathbb{R}_i^{\lambda} \oplus \mathbb{R}_u^{\gamma}$ is chosen that maps a certain part of $\mathcal{S}$ to the coordinate planes of the inductors and capacitors, respectively. Now we use the map π^* to "lift" or "pull-back" Ω and G on the state space $\mathcal{S}$. This operation is local because there are situations where $\mathcal{S}$ is folded just like in fig. 6.1. In this case, there is more than one part of $\mathcal{S}$ that can be mapped to the same part of the coordinate planes. With respect to the local dynamics of a circuit, the following theorem is fundamental.

If the Ohmian space $\mathcal{O}$ is a smooth manifold, the Kirchhoffian space $\mathcal{K}$ and the Ohmian space $\mathcal{O}$ are transversal and a pullback map π^* exists such that a 1-form $\omega := \pi^*\Omega$ and a non-degenerated 2-tensor (bilinear map) $g := \pi^*G$ can be defined on $\mathcal{S}$, then there exists locally a unique vector field $X\colon \mathcal{S} \to T(\mathcal{S})$ which satisfies

$$g(X,Y) = \omega(Y) \tag{6.2}$$

for all smooth vector fields Y. With this locally defined vector field X we are able to define the (local) dynamics of a circuit by means of $\dot{\xi} = X \circ \xi$.

6.2.1 Singular Points and Jumps

There are several cases where a locally defined vector field X does not exist. If $\mathcal{S}$ is a smooth manifold, then it is essential that g is non-degenerated. The bilinear map $g := \pi^*G$ can be interpreted as an inner product such that the assumed non-degeneracy of g follows from the condition $g(X,Y) = 0$ for all $Y \Leftrightarrow X = 0$. Therefore a degeneracy of g results from defects of π^* or G. G is degenerated if $L(i)$ or $C(u)$ is zero for some i and u, respectively, where these nongeneric cases can be remodelled by parasitic reactances. A defect of π^* is related to a dependency of the dynamic variables. With respect to the Kirchhoffian space $\mathcal{K}$ a defect of π^* corresponds to loops of capacitors and independent voltage sources or so-called cut-sets of inductors and independent current sources. With respect to the Ohmian space $\mathcal{O}$ a defect of π^* is related to a zero of du_R/di_R or di_R/du_R such that above mentioned loops and meshes arise. Also in these cases a remodelling process is available in order to obtain a generic situation of the circuit dynamics. For further details the reader is left to Mathis [16].

These considerations can be discussed in a more concrete manner if circuit topology is included. For this purpose we have to restrict ourself to RLC circuits. Then interconnections of a circuit can be described by oriented graphs and its boundary and coboundary operators or assuming a coordinate system (a chart) by its incidence matrices. If we assume that a proper tree of a graph exists (i.e. a circuit including all capacitor branches and no inductor branches), then no so-called "forced degeneracies" arise. These forced degeneracies are defects of the dynamics related e. g. to meshes of capacitors and cut-sets of inductors.

It is shown by Ichiraku [17] that a point (i,u) of the state space $\mathcal{S}$ is a singular point if and only if the characteristic manifold $\mathcal{O}_R$ and the affine subspace $\mathcal{K}_R$ are not transverse at $(i_R,u_R) := \pi_R(\mathbb{R}^{2n})$ where π_R is the natural projection from

the embedding space $\mathbb{R}^{2n}$ to the currents and voltages of the resistors. $\mathcal{K}_R$ is the Kirchhoffian space and $\mathcal{O}_R$ is the Ohmian space of the resistive circuit obtained from the given one by open-circuitting all inductor branches and short-circuitting all capacitor branches.

In the following, we exclude forced degeneracies from our discussion (i.e. meshes of capacitors and cut-sets of inductors, as well as $L(i) = 0$ or $C(u) = 0$), which cause the dynamics to be degenerated [18].

6.3 Chart Representation of Circuits and Jump Phenomena

By choosing a suitable chart, the circuit equations can be considered as algebro-differential equations (DAEs) [3] in a semi explicit form:

$$\mathbf{C}(\mathbf{x})\dot{\mathbf{x}} = \mathbf{g}(\mathbf{x},\mathbf{y},\mathbf{z}) \qquad \mathbf{g}:\mathbb{R}^k \to \mathbb{R}^n \tag{6.3}$$

$$\mathbf{0} = \mathbf{f}(\mathbf{x},\mathbf{y},\mathbf{z}) \qquad \mathbf{f}:\mathbb{R}^k \to \mathbb{R}^m \tag{6.4}$$

The vector $\mathbf{x} \in \mathbb{R}^n$ corresponds to the capacitor voltages and inductor currents, $\mathbf{z} \in \mathbb{R}^\eta$ is the vector corresponding to independent voltage or current input sources (which can also be a function of time $\mathbf{z}(t)$) and $\mathbf{y} \in \mathbb{R}^m$ is a vector of additional voltages and currents. Here, η is the number of independent sources. The matrix $\mathbf{C}(\mathbf{x})$ is related to the dynamical elements and becomes a constant matrix for linear inductances and capacitances. The nonlinear vector field with respect to $\mathbf{x}$, $\mathbf{y}$ and $\mathbf{z}$ is represented by $\mathbf{g}$.

Now, we have to introduce the embedding space $\mathcal{E} = \mathbb{R}^k$ and define $\mathcal{S}$ as a subspace of $\mathcal{E}$. The solution set of the algebraic equations (6.4) represents the state space $\mathcal{S}$ of the circuit, whereas the differential equations (6.3) represent its dynamical behavior. The dimension k of the embedding space can be determined by $k = n + m + \eta$. The state space $\mathcal{S}$ has the dimension $l = n + \eta$ and the codimension is $m = k - l$.

6.3.1 Jumps in State Space

As mentioned in section 6.2.1, a generic dynamics of a circuit do not exist at points where the projection map π^* has singularities. Such singularities arise if the state space is folded, which would result in a jump of the transient solution from one point on $\mathcal{S}$ to another instantaneously. Considering that the energy of capacitors and the charge of inductors is preserved, the voltages across capacitances and currents through inductances have inertia through a jump process and do not change (i.e. the values of $\mathbf{x}$ do not change during the jump). Another restriction is the fixed value of $\mathbf{z}$ during a jump.

Then, with respect to the semi explicit DAE representation, the singular points are defined at points where the local solvability to $\mathbf{y}$ is not guaranteed. These points are specified by the following condition:

$$\det\left(\frac{\partial \mathbf{f}(\mathbf{x},\mathbf{y},\mathbf{z})}{\partial \mathbf{y}}\right) = 0 \text{ where } \mathbf{f}(\mathbf{x},\mathbf{y},\mathbf{z}) = \mathbf{0} \tag{6.5}$$

Therefore we assume eq. (6.5) to be the necessary jump condition (cf. [19] [20], [21]).

The zero set of all points fulfilling the $m+1$ algebraic equations specified by eq. (6.5) is called "jump-set" Γ and represents a $l-1$-dimensional subset of $\mathcal{S}$. Of course, the calculation of the solution set of this equation system is difficult. However, we are not interested in all roots of eq. (6.5), but only in the actual chosen jump point during a simulation. Hence, we trace the dynamics on $\mathcal{S}$ (specified by eq. (6.3) and (6.4)) till reaching a stopping point P_s. This stopping point is defined as a point, where the step size of the numerical solver reaches a lower boundary (which is related to the machine constant of the simulating computer). In the next step, we search for the "nearest" point on Γ (by choosing a suitable norm) and define it as actual jump point P_j (cf. Fig 6.2). Furthermore, we define a straight line ξ_s connecting P_s and P_j, which will be used for determining the hit point.

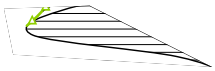

Fig. 6.2 Concept for jump point calculation; Γ: green triangles; trajectory: blue circles; ξ_s: red line

The sufficient jump condition is first given in a heuristic sense:
A point, which is specified by eq. (6.5) and whose neighborhood includes a Lyapunov stable and an unstable point, is called proper jump point P_j. The sufficient jump condition can be verified by calculating the eigenvalues λ_i of the characteristic equation

$$\det\left(\frac{\partial \mathbf{f}(\mathbf{x},\mathbf{y},\mathbf{z})}{\partial \mathbf{y}} - \lambda \cdot \mathbf{E}\right) = 0 \tag{6.6}$$

$$\lambda^m + \beta_{m-1} \cdot \lambda^{m-1} + \cdots + \beta_1 \cdot \lambda^1 + \beta_0 = 0\,, \tag{6.7}$$

where $\mathbf{E}$ is the identity matrix (cf. theory of discontinuous oscillators e.g. [21], [22]). If all λ_i of eq. (6.7) have negative real parts, the sufficient jump condition is not fulfilled and there are no proper jump points. The difference from the definition in this work to the one in the theory of discontinuous oscillators [21], [22] is, that we interpret $\mathbf{z}$ as variables and therefore extend the approach to all systems with fast switching behavior caused by a fold in their state space manifold and not only to autonomous circuits.

The jump-set Γ separate the state space manifold in a stable $\mathcal{S}^-$ and an unstable $\mathcal{S}^+$ part, which are defined by the real part of the eigenvalues

$$\mathcal{S}^- : \quad \Re e\{\lambda_i\} < 0, \quad \forall i \in N, i \leq k \tag{6.8}$$

$$\mathcal{S}^+ : \quad \Re e\{\lambda_i\} > 0, \quad \exists i \in N, i \leq k\,. \tag{6.9}$$

By crossing the jump-set Γ between stable and unstable region, there appears either one real positive λ or a pair of conjugate complex λ_1, λ_2 with positive real parts. The appearance of more than two λ_i with positive real parts is uncommon and will not be analyzed [21]. In the following we will restrict ourself to the case, where only one real positive λ appears. Then, for points on Γ there is only one eigenvalue equal to zero. As a result the constant term of eq. (6.7) (which corresponds to eq. (6.5) $\beta_0 = \det\left(\partial_{\mathbf{y}}\mathbf{f}(\mathbf{x},\mathbf{y},\mathbf{z})\right)$) is equal to zero. Therefore, the necessary and sufficient jump condition can be tested by the zero crossing of the determinant (6.5).

Because of the fixed values of $\mathbf{x}$ and $\mathbf{z}$ during the jump, the jump takes place in a tangential space of $\mathbb{R}^m$, which corresponds to the coordinate space of $\mathbf{y}$. In the following, the jump space will be denoted by $\mathcal{JS}$. Because we introduced the embedding space, the hit point P_h can be calculated by the intersection of the jump space defined in the jump point and the state space, excluding the jump point ($P_h \in (\mathcal{JS}_{P_j} \cap \mathcal{S}) \setminus \Gamma$). Therewith, it is guaranteed that the values of $\mathbf{x}_j = \mathbf{x}_h$ and $\mathbf{z}_j = \mathbf{z}_h$ before and after the jump are the same. Hence the corresponding "hit-set" is the intersection of the "bundle" of all jump spaces at points of the jump-set and the state space $\mathcal{S}$.

The conditions for fast switching can be summarized as follows:

- The necessary and sufficient jump condition have to be fulfilled: This can be tested by the zero crossing of $\det\left(\partial_{\mathbf{y}}\mathbf{f}(\mathbf{x},\mathbf{y},\mathbf{z})\right)$ for points on $\mathcal{S}$.
- The trajectories hit again the manifold: The intersection of $\mathcal{JS}$ and $\mathcal{S}$ have another solution than the jump point itself, i.e. $(\mathcal{JS}_{P_j} \cap \mathcal{S}) \setminus \Gamma$ is transversal and not empty.

6.3.2 Determining the State Space

If one is interested in plotting the state space in a certain area, the following considerations are necessary. Since there are electronic circuits like e.g. the Schmitt Trigger circuit which exhibits a fold respectively the independent input sources $\mathbf{z}$, $\mathcal{S}$ is "near the jump" not unique with respect to $\mathbf{z}$. Thus, for the determination of $\mathcal{S}$, one has to interpret $\mathbf{z}$ as variables and not as a constant or time dependent input value. Furthermore, also the values of $\mathbf{x}$ are fixed during the jump. As a consequence $\mathcal{S}$ is "near the jump" unique with respect to $\mathbf{y}$ and not unique with respect to $\mathbf{x}$ and $\mathbf{z}$ (cf. Fig. 6.3). So, by specifying l components of $\mathbf{y}$, one can determine $\mathcal{S}$. During the determination of $\mathcal{S}$, the determinant criterion can be checked by the local evaluation of eq. (6.5) yielding the jump-set. Nevertheless, there are circuits (e.g. the series connection of resonant tunneling diodes), where the state space is not unique to any coordinate. In this case, the determination of $\mathcal{S}$ is not possible with the method described here. One possibility could be the usage of geodesic coordinates.

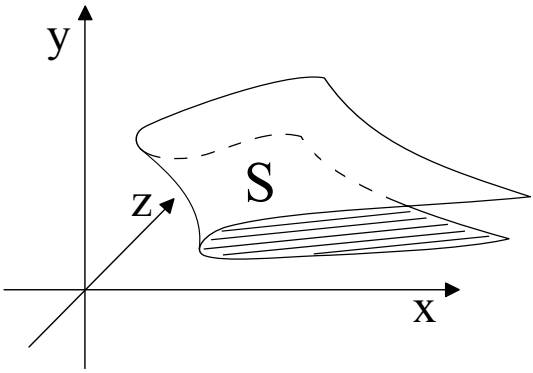

Fig. 6.3 Uniqueness of the state space with respect to **y**

6.3.3 Transient Solution and Hit Point Calculation

For the computation of the transient solution, of course, the time dependency of the input sources $\mathbf{z}(t)$ has to be taken into account. Since the dynamics is not defined at points of the jump-set, it increases very fast nearby the jump-set while tracing it. Therefore we have defined a stopping criterion, which compares the actual step size of the numerical integrator with a lower boundary (see section 6.3.1). When the step size reaches this boundary, the integration is stopped at a point P_s. From here, the jump point P_j is calculated as described in section 6.3.1. Then, the corresponding hit-point P_h will be calculated by the intersection of the jump space $\mathcal{JS}$ defined in a point $P_{j'}$ and $\mathcal{S}$ (cf. Fig. 6.4; here $\mathcal{JS}$ is one-dimensional). The point $P_{j'}$ is chosen not to be the actual jump point P_j which lies in $\mathcal{S}$. After calculating the jump point P_j, we use the distance Δ from P_s to P_j on ξ_s to calculate $P_{j'}$ (see Fig. 6.4). Thereby, we make sure that $P_{j'}$ does not lie in $\mathcal{S}$ and the numerical solver is able to find a unique hit-point $P_{h'}$. If one is interested to get a more exact numerical solution of P_h, one can calculate the solution of the intersection of $\mathcal{JS}_{P_j} \cap \mathcal{S}$ with the initial value $P_{h'}$. But, as we will see in section 6.5, the hit point $P_{h'}$ is comparable to the hit point of a regularized circuit. From P_h the dynamics can be traced, till reaching the jump-set again.

Fig. 6.4 Concept for hit point calculation

6.4 Adaption of the Geometric Approach to MNA Based System of Equations

Common circuit simulators (e.g. SPICE) are based on MNA, which leads in the description of electronic circuits to a high dimensional system of equations. To apply the methods described in section 6.3, several modifications to the classical MNA are necessary [23].

6.4.1 Modification of the System of Equations

From a given netlist of an electronic circuit, we obtain the system of equations (6.10), which results from applying the MNA stamps [24].

$$\tilde{\mathbf{C}}(\mathbf{n})\dot{\mathbf{n}} + \tilde{\mathbf{G}}\mathbf{n} = \tilde{\mathbf{B}}\mathbf{u}(\mathbf{n},t) \tag{6.10}$$

$\tilde{\mathbf{C}}(\mathbf{n})$ is the matrix related to the dynamical elements which is, for typical circuits, a singular matrix. If there are nonlinear capacitances or inductances, one approach is to separate $\tilde{\mathbf{C}}(\mathbf{n})$ in a linear and a nonlinear part. But, for simplicity, in the following we only consider linear inductances and capacitances, so that $\tilde{\mathbf{C}}$ is a constant matrix. $\tilde{\mathbf{G}}$ is the coefficient matrix related to the non-dynamic elements and $\tilde{\mathbf{B}}$ is the coefficient matrix related to the input sources. The vector $\mathbf{n}$ contains node voltages and currents including at least the currents i_L through inductances. The nonlinear elements are considered as nonlinear dependent current or voltage sources and summarized together with the input sources in the vector $\mathbf{u}(\mathbf{n},t)$. Now, we have to modify the system of equations to apply the methods described earlier.

Since we exclude forced degeneracies from our discussion (i.e. meshes of capacitors and cut-sets of inductors, as well as $L(i) = 0$ or $C(u) = 0$), the rank r_C of $\tilde{\mathbf{C}}$ is equal to the number of capacitances and inductances. Therefore, we add the rows of $\tilde{\mathbf{C}}$, so that there are only r_C non zero rows remaining. Simultaneously, we manipulate the matrices $\tilde{\mathbf{G}}$ and $\tilde{\mathbf{B}}$ in the same manner, yielding:

$$\mathbf{C}^*\dot{\mathbf{n}} + \mathbf{G}^*\mathbf{n} = \mathbf{B}^*\mathbf{u}(\mathbf{n},t)\,. \tag{6.11}$$

By now, the vector $\mathbf{n}$ includes only node voltages and currents. To distinct $\mathbf{n}$ in conserved quantities and non conserved quantities, i.e. in $\mathbf{x}$ and $\mathbf{y}$, we have to insert the capacitor voltages. Therefore, we add algebraic equations which describe the relations between capacitor voltages and the corresponding node voltages (e.g. $U_{C1} = \varphi_{n3} - \varphi_{n7}$) to the system of equations. We summarize all capacitor voltages and inductor currents in the vector $\mathbf{x}$ and all additional node voltages and currents in the vector $\mathbf{y}$. The input vector $\mathbf{u}$ is divided into nonlinear sources $\mathbf{h}(\mathbf{x},\mathbf{y})$, constant bias sources $\mathbf{u_0}$ and independent input sources $\mathbf{z}$ (which can also be a function of time $\mathbf{z}(t)$). The further modifications leads to the system of equations:

$$\mathbf{C}\begin{pmatrix}\dot{\mathbf{x}}\\ \dot{\mathbf{y}}\end{pmatrix}+\mathbf{G}\begin{pmatrix}\mathbf{x}\\ \mathbf{y}\end{pmatrix}=\mathbf{B}\begin{pmatrix}\mathbf{h}(\mathbf{x},\mathbf{y})\\ \mathbf{u_0}\\ \mathbf{z}\end{pmatrix}, \tag{6.12}$$

which can be formulated as semi explicit system of equations:

$$\begin{pmatrix}\mathbf{C}_{11} & 0\\ 0 & 0\end{pmatrix}\begin{pmatrix}\dot{\mathbf{x}}\\ \dot{\mathbf{y}}\end{pmatrix}+\begin{pmatrix}\mathbf{G}_{11} & \mathbf{G}_{12}\\ \mathbf{G}_{21} & \mathbf{G}_{22}\end{pmatrix}\begin{pmatrix}\mathbf{x}\\ \mathbf{y}\end{pmatrix}=$$
$$\begin{pmatrix}\mathbf{B}_{11} & \mathbf{B}_{12} & \mathbf{B}_{13}\\ \mathbf{B}_{21} & \mathbf{B}_{22} & \mathbf{B}_{23}\end{pmatrix}\begin{pmatrix}\mathbf{h}(\mathbf{x},\mathbf{y})\\ \mathbf{u_0}\\ \mathbf{z}\end{pmatrix}. \tag{6.13}$$

Furthermore, it becomes apparent that the addition of branch voltages is suitable. These additional voltages are stored in the vector $\mathbf{b}$, which can be determined by $\mathbf{b}=\mathbf{L}\cdot\mathbf{y}$, where $\mathbf{L}$ is the matrix relating the node potentials to their branch voltage.

6.5 Application on Two Simple Example Circuits

The described concept is illustrated on an emitter coupled multivibrator shown in Fig. 6.5 and on a Schmitt Trigger shown in Fig. 6.13. To analyze the circuits, we use the Ebers-Moll model in forward mode. For the comparison of our non-regularized solution with the solution of the regularized system, the parasitic base-emitter capacitances C_{reg} parallel to the diodes D_1 and D_2 were added.

6.5.1 Emitter Coupled Multivibrator

The design parameters are $R=500\Omega, R_i=100k\Omega, C=33nF, I_S=7fA, V_T=26mV$ and $\alpha_F=0.99$. For the simulation we use a constant bias voltage $U_0=5V$ and a constant bias current $I_1=I_2=0.26mA$.

The resulting vector $\mathbf{u}$ can be found in Fig. 6.6, the vector $\mathbf{n}$ in Fig. 6.7 and the matrix dimension in Fig. 6.8. Here the dimension of the embedding space is $k=9$ and because $r_C=1$, we have to split one dynamic equation from the algebraic ones. The state space is one-dimensional ($l=k-m=1$) and the codimension is $m=8$. To display $\mathcal{S}$, we assign the diode voltages to the corresponding node voltages $U_{D1}=\varphi_{n5}-\varphi_{n1}$ and $U_{D2}=\varphi_{n6}-\varphi_{n2}$. In Fig. 6.9 the state space (blue) in the coordinate system $U_{D1}-U_{D2}-U_C$ is shown. The associated jump is represented by the red line (triangles) and, for comparison, the transient solution of the regularized system is shown by the green line (circles).

In Fig. 6.10 the transient solutions of the circuit in relation to different regularization capacitances ϵ is shown. As one can see, $P_{jump,reg}$ and $P_{hit,reg}$ approaches for $\epsilon\to 0$ the non regularized case. $P_{jump,reg}$ represents the point where the transient solution significantly comes off $\mathcal{S}$ and $P_{hit,reg}$ represents the point, where the transient solution first proceeds in the near of $\mathcal{S}$. Furthermore one can see, that the overshoots of the transient responses after reaching the stable part of $\mathcal{S}$ again is independent from ϵ.

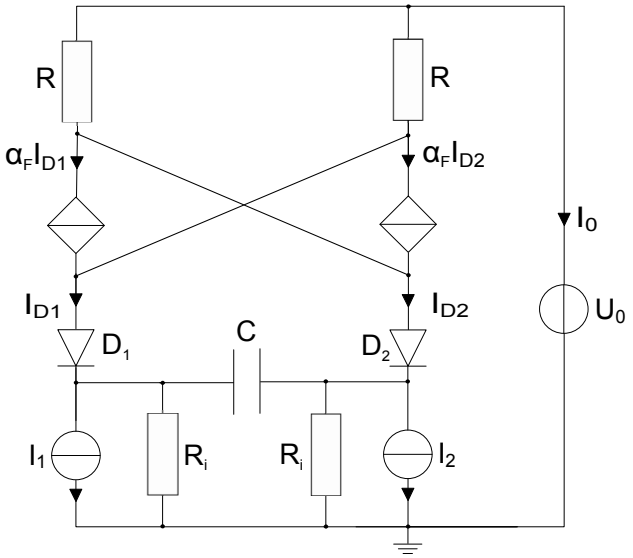

Fig. 6.5 Emitter coupled multivibrator

$$\mathbf{u} = \begin{bmatrix} I_{D1} \\ I_{D2} \\ I_1 \\ I_2 \\ U_{VS} \end{bmatrix} = \begin{bmatrix} 7 \cdot 10^{-15} \cdot (e^{\frac{\varphi_{n5} - \varphi_{n1}}{26 \cdot 10^{-3}}} - 1) \\ 7 \cdot 10^{-15} \cdot (e^{\frac{\varphi_{n6} - \varphi_{n2}}{26 \cdot 10^{-3}}} - 1) \\ 0.00026 \\ 0.00026 \\ 5 \end{bmatrix}$$

Fig. 6.6 Vector **u** including input sources and nonlinear dependent sources

$$\mathbf{n} = \begin{bmatrix} \mathbf{x} \\ \mathbf{y} \end{bmatrix} = \begin{bmatrix} U_C \\ \varphi_{n7} \\ \varphi_{n6} \\ \varphi_{n5} \\ \varphi_{n1} \\ \varphi_{n2} \\ I_{VS} \\ I_{D1} \\ I_{D2} \end{bmatrix}$$

Fig. 6.7 Vector **n** including **x** and **y**

matrix	rows	columns
C	9	9
B	9	5
G	9	9
L	2	8

Fig. 6.8 Matrix dimensions

By comparing Fig. 6.11 and 6.12, one can see, that our concept enables a simulation without regularization. Of course, the peaking during the switching process does not exist in our solution, but the main problem, namely the functionality of the circuit, is guaranteed.

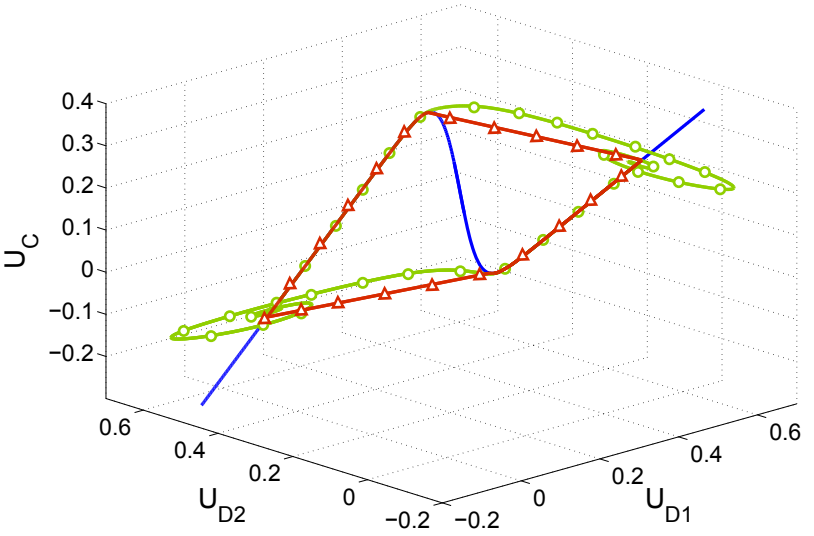

Fig. 6.9 State space (blue) in $U_{D1} - U_{D2} - U_C$ coordinate system; non-regularized jump solution (red triangles); regularized solution (green circles) $C_{reg} = 500pF$

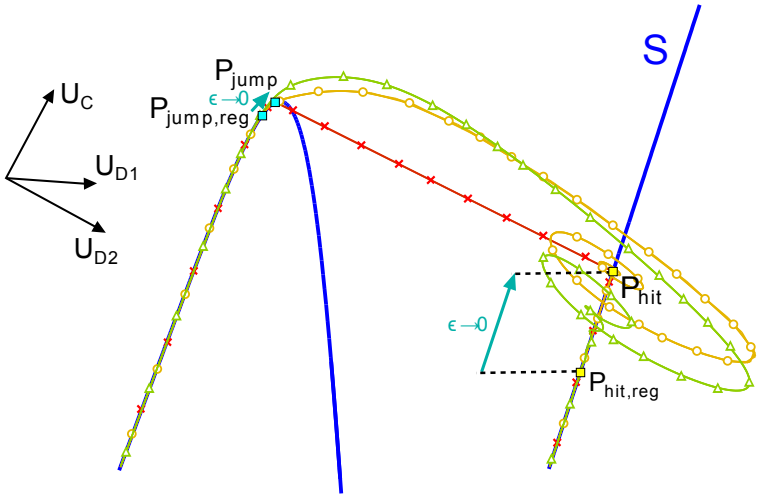

Fig. 6.10 Transient solution in relation to different regularization capacitances $C_{reg} = \epsilon$ $C_{reg} = 900nF$ (green triangles), $C_{reg} = 10nF$ (yellow circles) and $C_{reg} = 0$ (red crosses)

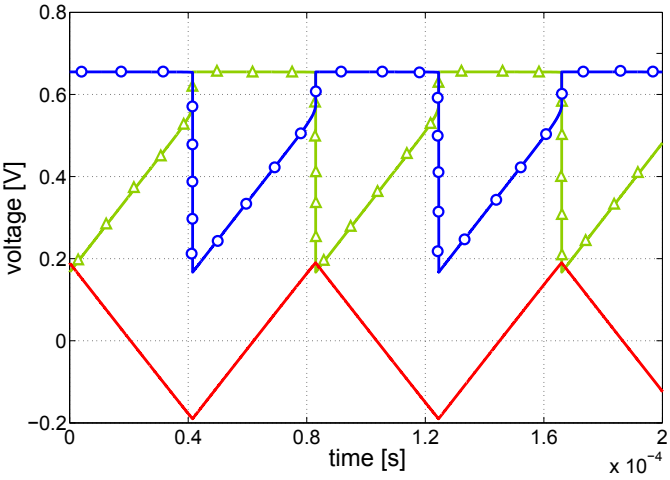

Fig. 6.11 Transient solution of non regularized multivibrator; U_{D1} (blue circles), U_{D2} (green triangles) and U_C (red)

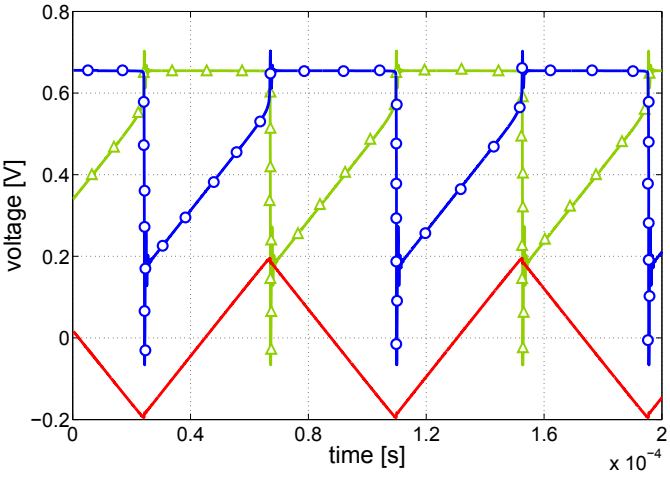

Fig. 6.12 Transient solution of regularized multivibrator $C_{reg} = 500pF$; U_{D1} (blue circles), U_{D2} (green triangles) and U_C (red)

6.5.2 Schmitt Trigger

The design parameters are $R_{C1} = R_{C2} = 1k\Omega, R_e = 100\Omega, R_1 = 8.2k\Omega, R_2 = 2.7k\Omega, R_V = 4.7k\Omega, I_S = 6.734fA, V_T = 26mV$ and $\alpha_F = 0.99$. For the simulation we use a constant bias voltage $U_0 = 10V$.

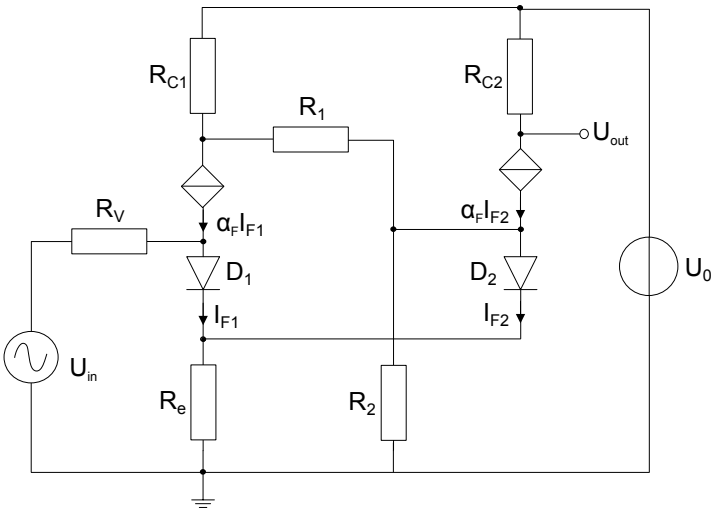

Fig. 6.13 Schmitt Trigger

$$\mathbf{u} = \begin{bmatrix} I_{D1} \\ I_{D2} \\ U_{V_1} \\ U_{IN} \end{bmatrix} = \begin{bmatrix} 6.734 \cdot 10^{-15} \cdot (e^{\frac{\varphi_{N6} - \varphi_{N7}}{26 \cdot 10^{-3}}} - 1) \\ 6.734 \cdot 10^{-15} \cdot (e^{\frac{\varphi_{N4} - \varphi_{N7}}{26 \cdot 10^{-3}}} - 1) \\ 10 \\ 1.5 + 1.5 \cdot (sin(2 \cdot \pi \cdot 1000 \cdot t)) \end{bmatrix}$$

Fig. 6.14 Vector **u** including input sources and nonlinear dependent sources

$$\mathbf{n} = \begin{bmatrix} \mathbf{x} \\ \mathbf{y} \end{bmatrix} = \begin{bmatrix} \varphi_{N1} \\ \varphi_{N2} \\ \varphi_{N6} \\ \varphi_{N5} \\ \varphi_{N4} \\ \varphi_{N3} \\ \varphi_{N7} \\ I_{V_1} \\ I_{V_{IN}} \\ I_{D1} \\ I_{D2} \end{bmatrix}$$

Fig. 6.15 Vector **n** including **x** and **y**

matrix	rows	columns
C	11	11
B	11	4
G	11	11
L	4	11

Fig. 6.16 Matrix dimensions

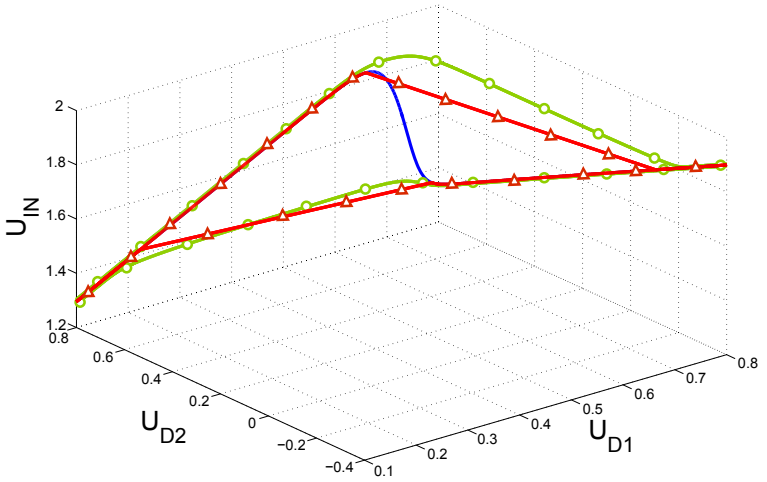

Fig. 6.17 State space (blue) in $U_{D1} - U_{D2} - U_{IN}$ coordinate system non-regularized jump solution (red triangles); regularized solution (green circles) $C_{reg} = 200pF$

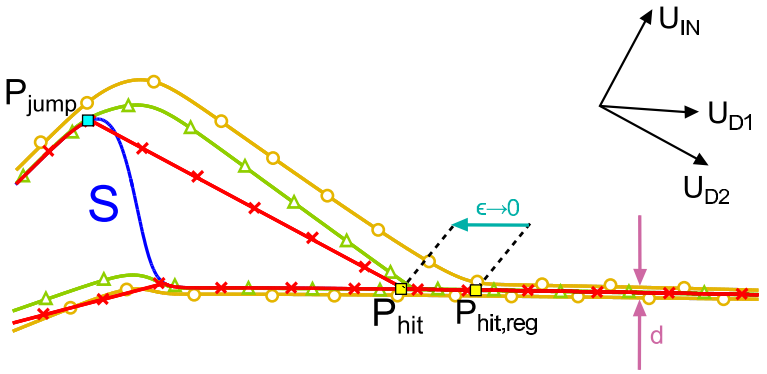

Fig. 6.18 Transient solution in relation to different regularization capacitances $C_{reg} = \epsilon$ $C_{reg} = 800pF$ (yellow circles), $C_{reg} = 50pF$ (green triangles) and $C_{reg} = 0$ (red crosses)

The resulting vector **u** can be found in Fig. 6.14, the vector **n** in Fig. 6.15 and the matrix dimension in Fig. 6.16. Here the dimension of the embedding space is $k = 12$ and there is one independent input voltage. Therefore state space is one-dimensional ($l = k - m = 1$) and the codimension is $m = 11$. To display $\mathcal{S}$, we assign the diode voltages to the corresponding node voltages $U_{D1} = \varphi_{n6} - \varphi_{n7}$ and $U_{D2} = \varphi_{n4} - \varphi_{n7}$. In Fig. 6.17 the state space (blue) in the coordinate system $U_{D1} - U_{D2} - U_{IN}$ is shown. The associated jump is represented by the red line (triangles) and, for comparison, the transient solution of the regularized system is shown by the green line (circles).

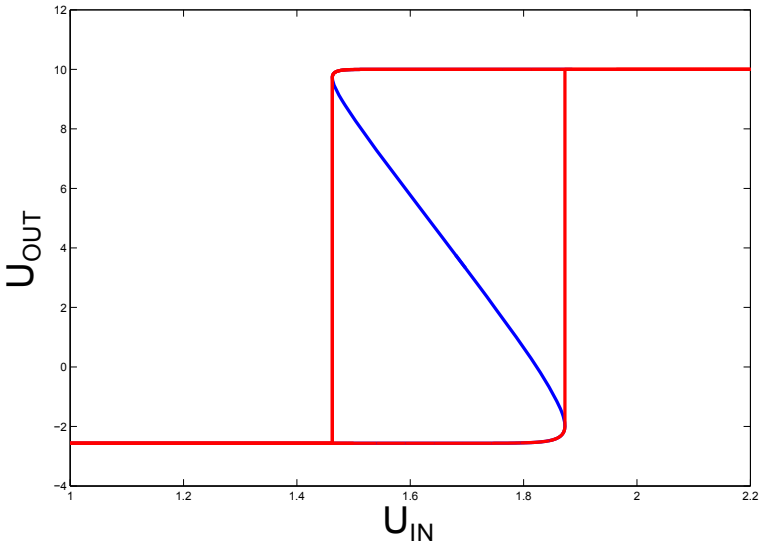

Fig. 6.19 Transfer characteristic in $U_{IN} - U_{OUT}$ coordinate system state space (blue), transient solution (red)

In Fig. 6.18 the transient solutions of the circuit in relation to different regularization capacitances ϵ is shown. Here, the regularized solution is far from the state space manifold and approaches for $\epsilon \to 0$ the non regularized case. Also the distance d from transient solution and $\mathcal{S}$ vanishes for $\epsilon \to 0$.

At the end, the known input output characteristic in form of a hysteresis is shown in Fig. 6.19.

6.6 Conclusion

In this article we have described why certain circuits with jumps sometimes require adding regularizing capacitors or inductors. We have given a geometric interpretation of jumps in state space and formulated a concrete local criterion to check if a circuit's state space manifold exhibits a fold. With our approach, it will not be necessary to add a regularization to get the transient solutions of a circuit. Furthermore we have shown, for the first time, a complete concept for adapting this geometric approach to a system of equations based on MNA. Therefore, the developed concept can be implemented in an MNA based circuit simulator like SPICE. Finally we have proven the functionality of our concept by numerical results of two BJT circuits. In a further work [25], we have adapted the non MNA based geometric approach to MOS circuits, where the EKV model is used as equivalent circuit diagram. However, the developed theory presented in this paper can be adapted to any electronic circuit containing a fold in their state space.

Acknowledgements. The authors would like to thank the German Research Foundation (DFG) for the financial support.

References

1. IEEE Solid-State Circuits Magazine, 3(2) (2011)
2. Sandberg, I.W., Shichman, H.: Numerical integration of systems of stiff nonlinear differential equations. Bell Syst. Tech. J. 47, 511–527 (1968)
3. Gear, W.: Simultaneous numerical solution of differential-algebraic equations. IEEE Transactions on Circuit Theory CT-18(1), 89–95 (1971)
4. Ihrig, E.: The regularization of nonlinear electrical circuits. Proceedings of the American Mathematical Society 47(1), 179–183 (1975)
5. Sastry, S., Desoer, C.: Jump behavior of circuits and systems. IEEE Transactions on Circuits and Systems 28(12), 1109–1124 (1981)
6. Chua, L.: Dynamic nonlinear networks: State-of-the-art. IEEE Transactions on Circuits and Systems CAS-27(11), 1059–1087 (1980)
7. Venkatasubramanian, V.: Singularity induced bifurcation and the van der pol oscillator. IEEE Transactions on Circuits and Systems I: Fundamental Theory and Applications 41(11), 765–769 (1994)
8. Tikhonov, A.N., Vasil'eva, A.B., Sveshnikov, A.G.: Differential Equations. Springer, Heidelberg (1985)
9. Knorrenschild, M.: Differential/algebraic equations as stiff ordinary differential equations. SIAM J. Numer. Anal. 29, 1694–1715 (1992), http://dx.doi.org/10.1137/0729096
10. Thiessen, T., Gutschke, M., Blanke, P., Mathis, W., Wolter, F.-E.: A numerical approach for nonlinear dynamical circuits with jumps. In: 20th European Conference on Circuit Theory and Design, ECCTD 2011 (2011)
11. Thiessen, T., Gutschke, M., Blanke, P., Mathis, W., Wolter, F.-E.: Differential Geometric Methods for Jump Effects in MOS Systems (presented). In: 2012 IEEE International Symposium on Circuits and Systems, ISCAS 2012 (2012)
12. Smale, S.: On the mathematical foundation of electrical circuit theory. Journ. Differential Geometry 7(1-2), 193–210 (1972)
13. Mathis, W.: Geometric Theory of Nonlinear Dynamical Networks. In: Moreno-Díaz, R., Pichler, F. (eds.) EUROCAST 1991. LNCS, vol. 585, pp. 52–65. Springer, Heidelberg (1992)
14. Thiessen, T., Mathis: Geometric Dynamics of Nonlinear Circuits and Jump Effects. International Journal of Computations & Mathematics in Electrical & Electronic Engineering (Compel 2011) 30(4), 1307–1318 (2011)
15. Guillemin, V., Pollack, A.: Differential Topology. Prentice-Hall, Inc., Englewoods Cliffs (1974)
16. Mathis, W.: Theorie nichtlinearer Netzwerke. Springer, New York (1987)
17. Ichiraku, S.: On singular points of electrical circuits. Yokohama Mathematical Journal 26, 151–156 (1978)
18. Ichiraku, S.: Connecting Electrical Circuits: Transversality and Well-Posedness. Yokohama Mathematical Journal 27, 111–126 (1979)
19. Tchizawa, K.: An Analysis of Nonlinear Systems with Respect to Jump. Yokohama Mathematical Journal 32, 203–214 (1984)
20. Rozov, N.K.: Asymptotic theory of two-dimensional relaxation self-oscillating system. Mathematical Notes 37, 71–77 (1985)

21. Andronov, A., Vitt, A., Khaĭkin, S., Fishwick, W.: Theory of oscillators. Dover books on electronics, electricity, electrical engineering. Dover (1987)
22. Mishchenko, E.F., Rozov, N.K.: Differential Equations with Small Parameters and Relaxation Oscillators. Plenum Press, New York (1980)
23. Thiessen, T., Plönnigs, S., Mathis, W.: A Geometric MNA Based Approach for Circuits with Fast Switching Behavior (presented). In: 2012 IEEE International Symposium on Circuits and Systems, ISCAS 2012 (2012)
24. Vlach, J., Singhal, K.: Computer Methods for Circuit Analysis and Design. Springer, New York (1993)
25. Sarangapani, P., Thiessen, T., Mathis, W.: Differential algebraic equations of mos circuits and jump behavior (accepted). Advances in Radio Science